

Patterns of the fractal dimension evolution of magneto-optical images of magnets after exposure to a pulsed field

© A.D. Zigert, N.B. Kuz'min, E.M. Semenova, A.I. Ivanova, S.A. Tretyakov, N.Yu. Sdobnyakov[¶]

Tver State University,
Tver, Russia

[¶] E-mail: nsdobnyakov@mail.ru

Received May 12, 2023

Revised July 11, 2023

Accepted October 30, 2023

The results of fractal analysis of images of the surface of a permanent magnet NdFeB (N35 brand) obtained by the polar Kerr effect method using an indicator bismuth-containing ferrite-garnet film after magnetization reversal by a pulsed field of 0.1–2 T are presented. Two different methods of changing the magnetic field are used: sequential change in the magnitude of the magnetic pulse and magnetization to saturation before each acting pulse. A correlation between the form of the field dependences of the fractal dimension of the profile of magneto-optical images of the magnet surface $D_L(H)$ and the corresponding dependences $M_r(H)$ is established. The obtained data are compared with the results of a similar fractal analysis of the KC37 (SmCo) magnet.

Keywords: fractal dimension, remanence, field dependences, Kerr effect, ferrite-garnet film.

DOI: 10.61011/PSS.2023.12.57657.5091k

1. Introduction

Currently, fractal analysis is widely used in materials science to describe and compare structures with complex geometries. In [1–3] the fractal dimension is used to describe the surface structure of magnetic materials at the nano- and microlevel, followed by establishing correlations with their hysteresis characteristics. The authors [4], while studying the evolution of the labyrinth domain structure (DS) of magnetic materials, described the morphogenesis of the labyrinth DS in external magnetic field, suggesting that each of its stages corresponds to a certain value of the fractal dimension. In development of the paper [3] in [5] the results were presented of fractal analysis of magneto-optical (MO) images of the surface of a permanent magnet (PM) KC37, visualized using an indicator bismuth-containing ferrite-garnet film after remagnetization by a pulsed field 0.1–1.5 T. The obtained dependences of the relative residual magnetization on the magnitude of the external pulsed field $M_r(H)$ were compared with the fractal dimension of MO images of the magnet surface after exposure to the pulsed field. A correlation was established between the type of field dependences of the fractal dimension of the profile of MO images of the magnet surface and the first derivative of the relative magnetization with respect to the field $dM_r(H)/dH$. Thus, it was shown that there is a relationship between the nature of the change in magnetization in pulsed field and the type of MO image analyzed using the apparatus of fractal geometry.

2. Experiment

Experimental methods and quantitative analysis described in papers [3,5] were applied in this study to obtain MO

images of the surface of PM NdFeB (grade N35) and their fractal analysis. The main magnetic characteristics of the studied PM N35 are: residual magnetic induction $B_r = 1.2$ T, maximum energy product $BH_{\max} = 281$ kJ/m³, which corresponds to typical characteristics of PM NdFeB, including grade N35 [7]. The magnet sample under study had the shape of a cylinder (height $h = 1$ mm, radius $r = 1$ mm), with the base in the basal plane, i.e. the axis of the PM texture is directed along the generatrix of the cylinder. The experiment on PM exposure to demagnetizing pulsed field and recording MO images is described in detail in [3]. In this paper an additional method of exposure to pulsed field was also used, which can be described by the following new scheme: before each PM exposure to the demagnetizing pulsed field, the sample was magnetized to saturation along the texture axis in pulsed field of 1.5 T. The pulse width was $40 \mu\text{s}$, the field induction varied from 0.25 to 1.5 T. Visualization of PM scattering fields was carried out in several seconds after the pulse using indicator uniaxial ferrite-garnet film using the polar Kerr effect method. The own labyrinth DS film does not make a significant contribution to the images, since its surface is completely magnetized in the magnetic field.

It is known that the apparatus of fractal geometry is an effective analysis tool in the case when the system behavior is analyzed under changing conditions based on the analysis of complex images [8–12]. Note that the earlier application of fractal geometry to line structure patterns of the multi-branched domains made it possible in [13] to determine the values D_L in the range 1.33–1.65 for garnet films. For ferrite-garnet film, within the framework of the described model of the remagnetization [14] the fractal domain clusters with $D_L \approx 1.7$ were obtained. For MO images obtained during remagnetization of PM KC37, in [5] the field dependences

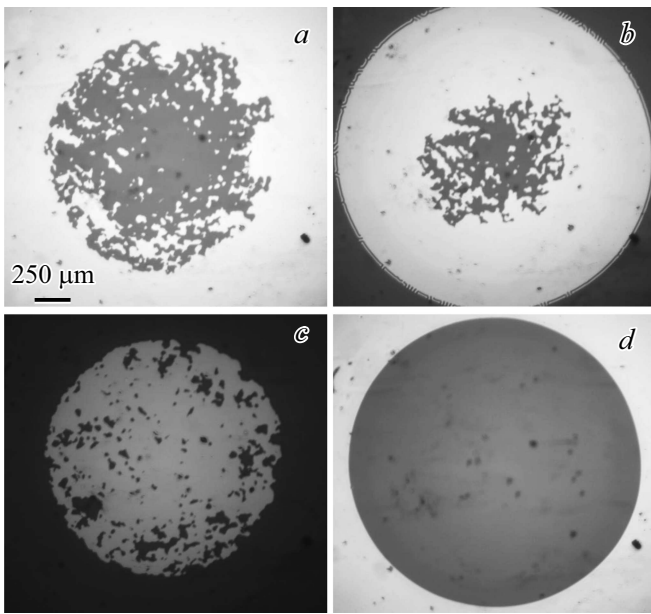


Figure 1. MO images of surface of permanent magnet grade N35 after exposure to pulsed magnetic field using the first demagnetization method: *a*) 1.025 T, *b*) 1.075 T; after exposure to the second method: *c*) 1.025 T, *d*) 1.25 T. Images are shown to the same scale.

of the fractal dimension with the maximum value $D_L \approx 1.82$ were determined in the vicinity of the coercive field.

In the present study as a result of experiments on remagnetization of PM N35 in pulsed field, two series of MO images were obtained. In the first experiment (the first demagnetization method), the PM magnetized to saturation was successively exposed to magnetic field pulses of increasing magnitude in the opposite direction. After each demagnetizing pulse the MO image of the sample was recorded, image is formed by an indicator film (see Figure 1, *a* and *b*). A similar experiment was performed in [3] on samples of the KC37 magnet. In the second experiment (second demagnetization method), the magnet was magnetized each time till saturation with the pulsed field and only after that was exposed to demagnetizing field in the opposite direction. Thus, in this case, the initial state of the PM before each exposure was the saturation state. After each demagnetizing pulse the state of the magnet was also recorded (see Figure 1, *c* and *d*).

To determine the relative magnetization and fractal dimension, the images were first contrasted to binary (black and white) one. Contrast was carried out in the open-source software product GIMP by setting the color level (this parameter varies from „0“ for black to „255“ corresponding to white color), below which all pixels are considered black, and above — white. For a series of MO images analyzed in this paper, the threshold values were chosen to be the same (color level = 120). The fractal dimension was determined by the method of cubes counting. The method for determining the fractal dimension is described in

detail in [1,3,5]. In the black-and-white images of Figure 1, areas of opposite contrast correspond to sections of the film magnetized in opposite directions. The saturation state corresponds to MO image where PM plane is uniformly colored and does not contain areas of reverse contrast. In this case, the demagnetized state corresponds to images where the number of white and black pixels coincides. Relative magnetization was estimated from the difference in areas of opposite contrast.

Figure 2 shows graphs of the field dependences of the relative magnetization and the corresponding dependences of the fractal dimension. Within each branch of the hysteresis loop $M_r(H)$, the fractal dimension D_L has an extremum near the coercive field, which is consistent with the data of the paper [5]. Moreover, the extreme course $D_L(H)$ is observed with both image acquisition methods. The maximum values $D_L \approx 1.82$ correspond to MO images with a complex branched configuration. Comparing the graphs $D_L(H)$ for PM N35 and KC37 [5], it can be noted

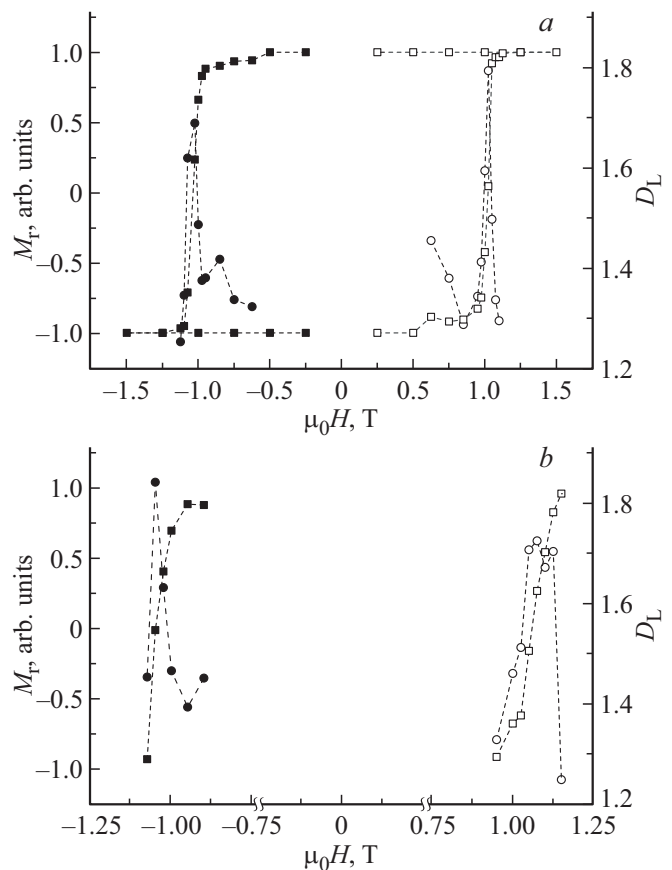


Figure 2. Dependences of the relative residual magnetization $M_r(H)$ (values are marked by squares) and the fractal dimension of the profile $D_L(H)$ (values are marked by circles) on the magnitude of the pulsed magnetic field *a*) at sequential change in the magnitude of the pulse (the designations correspond to the following directions of change in the external pulsed magnetic field: $\square - 0 \rightarrow H_{max} \rightarrow 0$; $\circ - 0 \rightarrow H_{max}$; $\bullet - 0 \rightarrow H_{min} \rightarrow 0$; $\bullet - 0 \rightarrow H_{min}$) and *b*) when exposed to pulses of various sizes from saturation (μ_0 — magnetic constant).

that on the dependence $D_L(H)$ of the first magnet the extremum has a narrower interval, which can be explained by a higher degree of rectangularity of the hysteresis loop of PM N35 compared to KC37. This difference is due to the fact that remagnetization in magnets of N35 type is carried out by the nucleation mechanism (for PM NdFeB it is described, for example, in [15]), and in KC37 — mainly due to the displacement of domain boundaries (for PM SmCo it is described, for example, in [16]).

3. Conclusion

Using the example of PM N35, as previously in the case of PM KC37 [5], data were obtained that allows one to assert the existence of a correlation between the patterns of behavior of the residual magnetization vs. magnitude of the external pulse field and the fractal dimension of the corresponding MO images. Considering that magnets N35 and KC37 are characterized by different mechanisms of remagnetization ([15,16]), the obtained result allows us to apply the described method of fractal analysis to wide class of permanent magnets. For example, in [17] for various compositions of PM NbFeB (the samples differ in doping additives), based on the analysis of images of the microstructure, reflecting the misorientation of magnet grains relative to the texture axis, obtained using scanning electron microscope in the reflected electron diffraction mode, values $D_L \approx 1.75–1.78$ for different orientations of the observation surface (in the basal and prismatic planes). At the same time, a composition was also found for which, regardless of the scales under study (from 60 to 120 μm), the fractal dimension reaches value of 1.82, which is in good agreement with both the results of this paper and the results of [5] for alternative PM.

Funding

The work was carried out with financial support from the Ministry of Science and Higher Education of the Russian Federation as part of the state assignment in the field of scientific activity (project No. 0817-2023-0006).

Conflict of interest

The authors declare that they have no conflict of interest.

References

- [1] A.D. Siegert, G.G. Dunaeva, N.Yu. Sdobnyakov. Physical and chemical aspects of the study of clusters, nanostructures and nanomaterials **13**, 134 (2021). (in Russian). <https://doi.org/10.26456/pcascnn/2021.13.134>
- [2] A.I. Ivanova, E.M. Semenova, G.G. Dunaeva, S.V. Ovcharenko, S.A. Tretyakov, A.D. Siegert. Physical and chemical aspects of the study of clusters, nanostructures and nanomaterials **12**, 103 (2020). (in Russian). <https://doi.org/10.26456/pcascnn/2020.12.103>
- [3] A.D. Siegert, E.M. Semenova, N.B. Kuzmin, N.Yu. Sdobnyakov. Physical and chemical aspects of the study of clusters, nanostructures and nanomaterials **14**, 101 (2022). (in Russian). <https://doi.org/10.26456/pcascnn/2022.14.101>
- [4] C. Bathany, M. Le Romancer, J.N. Armstrong, H.D. Chopra. Phys. Rev. B **82**, 18, 184411 (2010). <https://doi.org/10.1103/PhysRevB.82.184411>
- [5] A.D. Zigert, G.G. Dunaeva, E.M. Semenova, A.I. Ivanova, A.Yu. Karpenkov, N.Yu. Sdobnyakov. J. Supercond. Nov. Magn. **35**, 8, 2187 (2022). <https://doi.org/10.1007/s10948-022-06301-w>
- [6] M. Sagawa, S. Fujimura, N. Togawa, H. Yamamoto, Y. Matsuura. J. Appl. Phys. **55**, 6, 2083 (1984). <https://doi.org/10.1063/1.333572>
- [7] E. Diez-Jimenez, J.L. Perez-Diaz, C. Ferdeghini, F. Canepa, C. Bernini, C. Cristache, J. Sanchez-Garcia-Casarrubios, I. Valiente-Blanco, E.M. Ruiz-Navas, J.A. Martínez-Rojas. J. Magn. Mater. **451**, 549 (2017). <https://doi.org/10.1016/j.jmmm.2017.11.109>
- [8] F.V. Lisovskii, L.I. Lukashenko, E.G. Mansvetova. JETP Lett. **79**, 7, 352 (2004). <https://doi.org/10.1134/1.1765181>
- [9] J.P. Attané, M. Tissier, A. Marty, L. Vila. Phys. Rev. B **82**, 2, 024408 (2010). <https://doi.org/10.1103/PhysRevB.82.024408>
- [10] Yu.B. Kudasov, M.V. Logunov, R.V. Kozabaranov, I.V. Makarov, V.V. Platonov, O.M. Surdin, D.A. Maslov, A.S. Korshunov, E.Ya. Popov, A.S. Svetlov. Phys. Solid State **60**, 11, 2207 (2018). <https://doi.org/10.1134/S106378341811015X>
- [11] O.P. Polyakov, M.L. Akimov, P.A. Polyakov. Bull. Russ. Acad. Sci. **84**, 2, 166 (2020). <https://doi.org/10.3103/S106287382002029X>
- [12] D.-H. Kim, Y.-C. Cho, S.-B. Choe, S.-C. Shin. Appl. Phys. Lett. **82**, 21, 3698 (2003). <https://doi.org/10.1063/1.1578185>
- [13] B.-S. Han, D. Li, D.-J. Zheng, Y. Zhou. Phys. Rev. B **66**, 1, 014433 (2022). <https://doi.org/10.1103/PhysRevB.66.014433>
- [14] L.A. Dovbnya, D.E. Naumov, B.V. Khramov. Pis'ma v ZhETF **73**, 7, 410 (2001). (in Russian) [L.A. Dovbnya, D.E. Naumov, B.V. Khramov. JETP Lett. **73**, 7, 366 (2001). <https://doi.org/10.1134/1.1378121>]
- [15] D. Mukherjee, K. Danas. J. Appl. Phys. **125**, 3, 033902 (2019). <https://doi.org/10.1063/1.5051483>
- [16] H.R. Kirchmayr. J. Phys. D **29**, 11, 2763 (1996). <https://doi.org/10.1088/0022-3727/29/11/007>
- [17] Q. Sun, M. Zhu, J. Bai, Q. Wang. Fractal. Fractional **7**, 5, 393 (2023). <https://doi.org/10.3390/fractalfract7050393>

Translated by I.Mazurov